PROTEIN STRUCTURE REPORT

Crystal structure of rhodocytin, a ligand for the platelet-activating receptor CLEC-2

ALEKSANDRA A. WATSON,[1] JOHANNES A. EBLE,[2] AND CHRIS A. O'CALLAGHAN[1]

[1]Henry Wellcome Building for Molecular Physiology, University of Oxford, Oxford OX3 7BN, United Kingdom
[2]Center for Molecular Medicine, Department of Vascular Matrix Biology, Excellence Cluster Cardio-Pulmonary System, Frankfurt University Hospital, 60590 Frankfurt am Main, Germany

(RECEIVED April 10, 2008; FINAL REVISION June 14, 2008; ACCEPTED June 16, 2008)

Abstract

Binding of the snake venom protein rhodocytin to CLEC-2, a receptor on the surface of human platelets, initiates a signaling cascade leading to platelet activation and aggregation. We have previously solved the structure of CLEC-2. The 2.4 Å resolution crystal structure of rhodocytin presented here demonstrates that it is the first snake venom or other C-type lectin-like protein to assemble as a non-disulfide linked $(\alpha\beta)_2$ tetramer. Rhodocytin is highly adapted for interaction with CLEC-2 and displays a concave binding surface, which is highly complementary to the experimentally determined binding interface on CLEC-2. Using computational dynamic methods, surface electrostatic charge and hydrophobicity analyses, and protein–protein docking predictions, we propose that the $(\alpha\beta)_2$ rhodocytin tetramer induces clustering of CLEC-2 receptors on the platelet surface, which will trigger major signaling events resulting in platelet activation and aggregation.

Keywords: rhodocytin; C-type lectin; CLEC-2; CLEC1b; platelets; thrombosis; aggretin

The Malayan pit viper *Calloselasma rhodostoma* produces a potent venom protein, rhodocytin, which elicits powerful platelet activation and aggregation (Shin and Morita 1998). Rhodocytin was recently shown to be a ligand for CLEC-2, a newly identified receptor on the surface of platelets, and binding of rhodocytin to CLEC-2 triggers a novel platelet-signaling pathway (Suzuki-Inoue et al. 2006; Fuller et al. 2007). Rhodocytin binding leads to tyrosine phosphorylation in the cytoplasmic tail of CLEC-2, which promotes the binding of spleen tyrosine kinase (Syk), subsequent activation of PLCγ2, and platelet activation and aggregation (Suzuki-Inoue et al. 2006).

We have recently solved the structure of CLEC-2 and defined its binding interface with rhodocytin using site-directed mutagenesis and surface plasmon resonance binding studies (Watson and O'Callaghan 2005; Watson et al. 2007). The mechanism whereby rhodocytin triggers platelet aggregation is of great biomedical importance because a detailed knowledge of CLEC-2-mediated platelet activation could be of value in understanding and preventing platelet aggregation in thrombotic coronary and cerebral vascular disease, which are major causes of death and disability worldwide. We and others have recently characterized an endogenous ligand for CLEC-2, podoplanin (Suzuki-Inoue et al. 2007; Christou et al. 2008). Podoplanin does not have clear sequence similarity to rhodocytin, and its structure remains to be determined. Furthermore, understanding the rhodocytin–CLEC-2 interaction is of importance in its own right as snake envenomation affects over 2.5 million humans annually, causing more than 100,000 deaths (Chippaux 1998). The Malayan pit viper is a major cause of snakebite morbidity in large parts of Southeast Asia, with aberrant platelet function as one of its principal effects (Ho et al. 1986).

Reprint requests to: Chris O'Callaghan, Henry Wellcome Building for Molecular Physiology, University of Oxford, Roosevelt Drive, Oxford OX3 7BN, UK; e-mail: chris.ocallaghan@ndm.ox.ac.uk; fax: 44-1865-287787.

Article and publication are at http://www.proteinscience.org/cgi/doi/10.1110/ps.035568.108.

Results and Discussion

Rhodocytin is a non-disulfide linked $(\alpha\beta)_2$ tetramer

X-ray diffraction data to 2.4 Å resolution were obtained from crystals of rhodocytin and the structure was solved by molecular replacement (Table 1). The α- and β-subunits of rhodocytin share 39% sequence identity and are structurally homologous, displaying pseudosymmetry to one another. The αβ-heterodimer is stabilized by an interchain disulfide bond connecting C83 of the α-chain and C75 of the β-chain. Each subunit displays the canonical features of a C-type lectin-like fold, with two antiparallel β-sheets flanked by two α-helices, and three intramolecular disulfide bonds (Fig. 1A). However, the rhodocytin heterodimer is formed by domain swapping of the central extended loops of the α- and β-chains as observed in the structures of other snake venom C-type lectin-like proteins. While certain C-type lectin-like snake venom protein structures display an Mg^{2+}/Ca^{2+}-binding site, rhodocytin lacks the full set of cation-coordinating residues, and does not appear likely to interact with carbohydrate (Mizuno et al. 1997). The rhodocytin crystal structure can be superimposed onto our homology model of the rhodocytin αβ-heterodimer with a root-mean-square deviation (r.m.s.d.) of 1.23Å (Watson et al. 2007). No glycosylation was observed on either of the subunits of rhodocytin in the crystal structure, consistent with our bioinformatic, SDS-PAGE, and mass spectroscopy results (Watson et al. 2007).

Snake venom C-type lectin-like proteins have two homologous subunits, α and β, each ranging from 13–16 kDa in molecular weight. Of those crystallized to date, most, like the Factor X-binding protein (X-bp), are functionally active as discrete αβ-heterodimers (Mizuno et al. 2001). However, in both convulxin and flavocetin-A the αβ-heterodimers further multimerize to form cyclic, interchain disulfide-linked $(\alpha\beta)_4$ assemblies (Fukuda et al. 2000; Batuwangala et al. 2004). This higher order multimericity is believed to promote clustering of the cognate

Table 1. *Crystallographic data collection and refinement statistics*

Data collection	
Space group	*I*222
Unit-cell parameters (Å, °)	$a = 61.933$, $b = 89.368$, $c = 120.996$, $\alpha = \beta = \gamma = 90.000$
Wavelength (Å)	0.9762
Resolution (Å)	50.0–2.40 (2.49–2.40)
Redundancy	4.0 (3.7)
Completeness (%)	94.7 (80.8)
Total reflections	258,624
Unique reflections	13,367
R_{merge}[a] (%)	3.6 (11.6)
Average $I/\sigma(I)$	37.75 (7.05)
Refinement statistics	
Resolution (Å)	36.76–2.41
Average *B* factor (Å^2)	38.94
R_{cryst}/R_{free}[b] (%)	20.1/27.2
R.m.s.d. bonds (Å)	0.02
R.m.s.d. angles (°)	1.92
No. of non-hydrogen atoms	
Protein	2101
Water	45
Ions	5
Ramachandran plot regions (%)	
Favored residues	84.5
Allowed residues	15.6
Disallowed	0

Values in parentheses are for the highest resolution shell.
[a] $R_{merge} = \sum|I - \langle I\rangle|/\sum\langle I\rangle$ where I is the intensity of each reflection.
[b] $R_{cryst} = \sum||F_o| - |F_c||/\sum|F_o|$, where $|F_o|$ and $|F_c|$ are the observed and calculated structure-factor amplitudes, respectively. R_{free} is the cross-validation *R*-value calculated for 5% of the reflections omitted from the refinement.

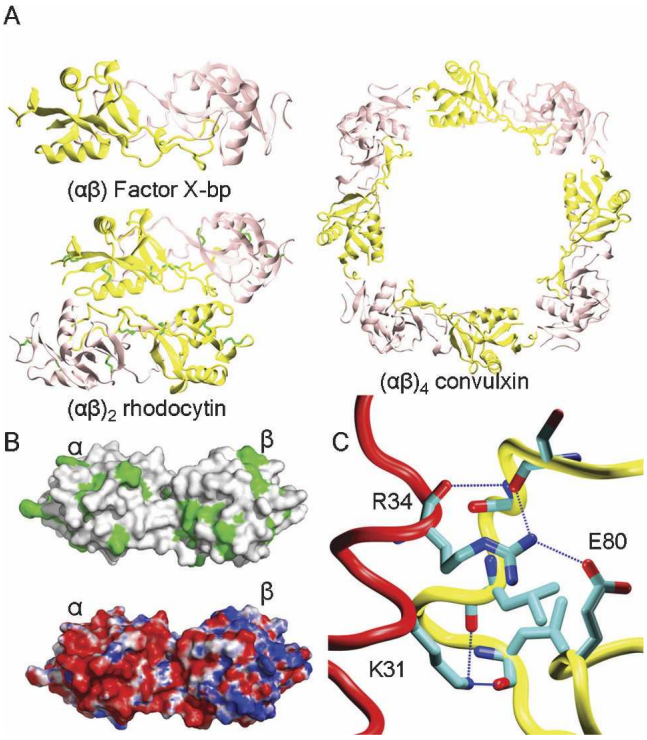

Figure 1. Rhodocytin is an $(\alpha\beta)_2$ tetrameric C-type lectin-like snake venom protein. (*A*) Rhodocytin forms a tetramer containing two copies of a disulfide linked αβ-heterodimer, whereas factor X-bp is dimeric, and convulxin is cyclic. α- and β-chains are colored yellow and pink, respectively. Disulfide bonds in rhodocytin are colored green. (*B*) Each image represents the molecular surface of one rhodocytin αβ-heterodimer at the interface that forms the tetramer. In the *upper* panel, the hydrophobic surface is colored green. In the *lower* panel, negatively and positively charged regions are colored red and blue, respectively, from −7 to +7 kTe. (*C*) Hydrogen bonds are shown as broken blue lines between residues of the two α-chains within the rhodocytin tetramer. For clarity, one α-chain is colored yellow and the other red. For residues involved in hydrogen bonds, carbon atoms are colored light blue, oxygen is red, and nitrogen is dark blue.

receptor on the platelet surface (GPVI for convulxin and GPIb for flavocetin-A), thus augmenting signal transduction activity (Fukuda et al. 2000; Batuwangala et al. 2004). The extent to which an isolated rhodocytin αβ-heterodimer could effectively activate CLEC-2 is not known, as the protein only exists in tetrameric form. However, in line with studies of the related protein convulxin, we would predict that its ability to do so would be severely diminished with respect to that of the endogenous tetrameric form (Kato et al. 2006). The octameric form $(\alpha\beta)_4$ of native convulxin displays a threefold increase in affinity for the platelet-activating glycoprotein receptor GPVI and has a 400-fold greater ability to induce platelet aggregation than the recombinant heterodimer.

The structure of rhodocytin demonstrates that it is the first $(\alpha\beta)_2$ tetrameric snake venom C-type lectin-like protein to have been crystallized (Fig. 1A). This is consistent with observations that rhodocytin is biologically active in its tetrameric 60 kDa form (Suzuki-Inoue et al. 2006). The two rhodocytin heterodimers within the tetramer are related by the following crystallographic symmetry operator: $x, -y, -z + (0\ 0\ 0)$. Symmetry is generally present in the arrangement of subunits in homodimeric and other oligomeric proteins (Brown 2006). For example, the venom protein flavocetin-A is an octamer made up of four αβ-heterodimers related by crystallographic fourfold symmetry (Fukuda et al. 2000). This form of tetrameric assembly has not been previously reported for members of the C-type lectin-like family of snake venoms and this interaction between the rhodocytin heterodimers is unique in that it is mediated by multiple noncovalent contacts between the α- and β-chains of opposing heterodimers. Figure 1B shows the molecular surface of one αβ-heterodimer as presented to its counterpart within the rhodocytin tetramer. This arrangement is stabilized by an electrostatic interaction between the highly negatively charged α-subunit and the positively charged elements of the β-subunit (Fig. 1B), and creates a buried surface area of 1998 Å^2. There are seven salt bridges formed in the assembly. The heterodimers are also linked by hydrogen bonds between residues K31 and L101, K31 and L98, and R34 and S94 of the two α-chains, respectively, and additionally by multiple favorable electrostatic interactions between charged residues surrounding nonpolar patches (Fig. 1B,C). Interchain salt bridges and dominant electrostatic interactions are made between the two heterodimers, with residue R34 on each α-chain forming salt bridges with residues E80 and E96 on the other α-chain. This unique tetramerization of rhodocytin is likely to have significant implications for the mechanism by which CLEC-2 activates platelets. For snake venom C-type lectin-like proteins which function as αβ-heterodimers, and whose purpose it is to sequester a soluble blood clotting factor ligand, such as Factor X-bp, increased binding avidity through multimeric binding and ligand clustering, are not high priorities in terms of biological function. However, for venoms such as rhodocytin, convulxin, and flavocetin-A, which bind surface receptors on platelets with intracellular cytoplasmic signaling elements, the capacity to cluster a ligand may be highly advantageous. Each rhodocytin subunit presents an equivalent binding surface for CLEC-2, and is positioned to accommodate multiple copies of CLEC-2. Thus, binding to rhodocytin may initiate higher order multimerization of CLEC-2 on the platelet surface, which in turn would localize its cytoplasmic signaling domains for phosphorylation and recognition by Syk, thereby promoting signal transduction.

Structural adaptations for CLEC-2 binding

All C-type lectin-like snake venom proteins exhibit a concave depression formed by the domain-swapped loop regions at the dimerization interface of the αβ-heterodimer. This curved surface is the ligand-binding site for all snake venom C-type lectin-like proteins that have been crystallized with their ligand and has been predicted to behave as such for all members of this family (Hirotsu et al. 2001; Mizuno et al. 2001). Figure 2A shows representations of the surface electrostatic charge distribution and exposed hydrophobicity of the predicted CLEC-2 binding groove of the rhodocytin tetramer. Consistent with our previous modeling, rhodocytin presents a predominantly negatively charged binding surface with discrete hydrophobic patches (Watson et al. 2007). The proposed binding cleft of the rhodocytin tetramer is negatively charged, mainly as a consequence of the multiple acidic residues at the surface of the α-subunits of each heterodimer. In terms of charge complementarity, this provides a favorable docking surface for the essentially positively charged binding face presented by CLEC-2 (Fig. 2A).

To explore the flexibility of rhodocytin as a tetrameric assembly, we performed computational dynamic analyses of the crystal structure. A covariance web for rhodocytin illustrates the strong positive correlation (denoted by red lines) between the motions of the two β-subunits, and to a lesser extent, between those of the two α-subunits (Fig. 2B). There is striking ''anticorrelation,'' or opposing directionality of the movements between α- and β-subunits both within and between heterodimers, represented by blue lines (Fig. 2B). This covariance web reveals a considerable degree of flexing permitted across the concave putative binding surface of the tetramer. The extent of this flexing motion is further demonstrated in the porcupine plot in Figure 2B. Here, the dominant motion of each Cα atom is represented by a cone, whose height and orientation represent the magnitude and direction of the motion, respectively (Barrett et al. 2004). This diagram emphasizes

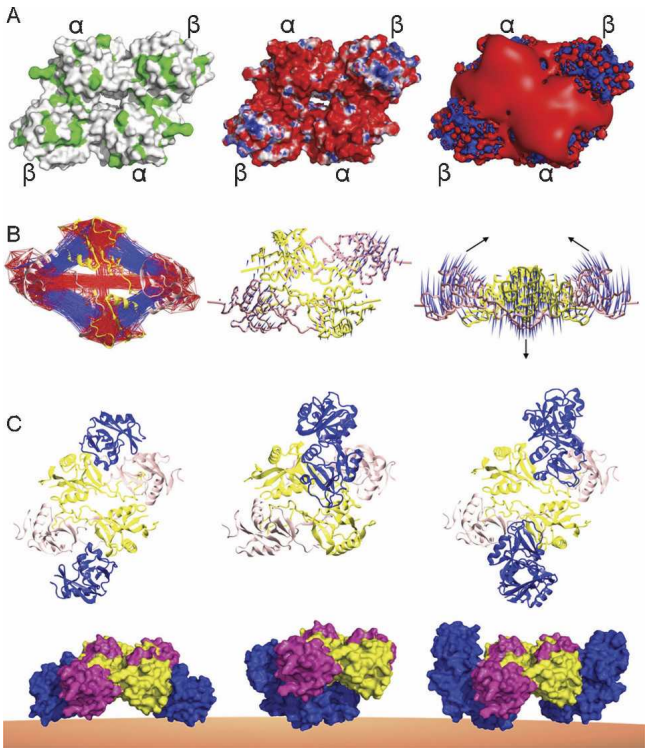

Figure 2. Structural adaptations of rhodocytin for CLEC-2 binding. (*A*) The *left* and *center* panels are molecular surface representations demonstrating surface hydrophobicity in green and electrostatic surface potential colored red to blue from −7 to +7 kTe. The *right* panel is an electrostatic isocontour representation scaled from −7 and +7 kTe. (*B*) Computational dynamic analysis of rhodocytin. The α- and β-chains are colored yellow and pink, respectively. The *left* image is a covariance web representation of rhodocytin: Red lines link pairs of Cα atoms, which undergo concerted motions, and blue lines link pairs of Cα atoms with uncorrelated motions. The *center* and *right* panels are porcupine plots of the principal mode of conformational variability of the Cα atoms calculated from a CONCOORD ensemble. Blue cones indicate the direction of motion, with the length proportional to the motion amplitude. The image on the *right* represents a 90° counterclockwise rotation of the central image about the *X*-axis. Black arrows emphasize the flexing motions caused by opposing movements of the α- and β-subunits around the binding groove of rhodocytin. (*C*) Tetrameric rhodocytin may promote clustering of CLEC-2 (colored blue) as two copies of monomeric CLEC-2 (*left*), one copy of dimeric CLEC-2 (*center*), or two copies of dimeric CLEC-2 (*right*). The rhodocytin-CLEC-2 complex is portrayed as a cartoon in the *upper* panel, and as molecular surfaces depicting how the complex might be arranged on the platelet surface (brown) *below*.

the capacity of the rhodocytin tetramer both to ''open'' the predominantly acidic binding surface to maximize its accessibility for engaging CLEC-2, and also to ''close around'' its ligand, once docked. This concert of potential motions is created by the opposing movements of the α- and β-subunits and indicates the likely mode of ligand binding by the rhodocytin tetramer. We have previously performed dynamic analyses of the structure of CLEC-2 (Watson et al. 2007). The motions available to the rhodocytin tetramer and to CLEC-2 are highly complementary, suggesting an interaction in which the long loop and flanking regions of CLEC-2 open out and broaden its binding surface, while rhodocytin similarly spreads and exposes its binding groove, and then grasps its bound ligand.

Rhodocytin may cluster multiple copies of CLEC-2 on the platelet surface

The structure of rhodocytin casts light on the mechanism by which binding of rhodocytin to the extracellular domain of CLEC-2 triggers intracellular phosphorylation events and ultimately platelet aggregation. The rhodocytin tetramer presents two copies of the concave binding surface created by each αβ-heterodimer, and may thus initiate higher order multimerization of CLEC-2 on the platelet surface. We propose that binding to rhodocytin brings the cytoplasmic signaling domains of several CLEC-2 molecules into closer proximity for phosphorylation and recognition by Syk, thereby facilitating signal transmission. We have previously shown that recombinant CLEC-2 is stable in solution as a monomer, and there is no suggestion of dimerization in the CLEC-2 crystal structure and lattice packing (Watson et al. 2007). Furthermore, this monomeric CLEC-2 binds rhodocytin with an affinity of 1.0 μM (Watson et al. 2007). The surface of the predicted binding groove of each heterodimeric subunit of rhodocytin has striking complementarity to that of the binding surface of CLEC-2 in terms of shape, electrostatic charge distribution, and location of nonpolar regions (Watson et al. 2007). In a model of this interaction, two copies of monomeric CLEC-2 can bind to each rhodocytin tetramer, giving a total buried surface area of 3200 $Å^2$ (Fig. 2C). However, ligand-induced dimerization is observed in signaling receptors, such as the receptor tyrosine kinases EGFR and PDGFR (Ji et al. 1998). Rhodocytin may similarly promote dimerization of CLEC-2 and recent studies suggest that murine CLEC-2 can dimerize under certain conditions (Xie et al. 2008). To investigate this possibility, we generated a molecular model of dimeric human CLEC-2, and simulated its interaction with rhodocytin (Fig. 2C). One copy of dimeric CLEC-2 can be docked onto the concave surface spread across the two αβ-heterodimers of rhodocytin burying 2305 $Å^2$ surface at the interface (Fig. 2C). An additional possibility is that one copy of the CLEC-2 dimer may interact with each of the two rhodocytin αβ-heterodimers with a total buried surface area of 4390 $Å^2$. All three of these model assemblies present feasible means by which a rhodocytin tetramer may multimerize CLEC-2 on the surface of platelets. In each, the potential flexibility of the rhodocytin tetramer may facilitate the recognition and docking interactions between ligand and

receptor, both by increasing the exposure of CLEC-2 to the individual αβ subunits and by maximizing the surface presented to CLEC-2 across both concave binding grooves (Fig. 2B,C). This set of motions potentially available to the rhodocytin tetramer may prolong its association with CLEC-2 by securing CLEC-2 in a position such that all electrostatic and hydrophobic contacts are optimized. Indeed, this model of a protracted association between rhodocytin and CLEC-2 offers a potential explanation as to how this toxin elicits such powerful platelet activation and aggregation in the absence of other stimuli and is consistent with the previously determined dissociation constant for the rhodocytin-CLEC-2 interaction of 1.0 μM (Watson et al. 2007). Further experimental studies involving the stimulation of platelets or cellular models with rhodocytin may be required to clarify which of these models most accurately represents the true rhodocytin-CLEC-2 interaction.

The crystal structure of rhodocytin and the dynamic, surface electrostatic charge, hydrophobicity, and shape complementarity protein-protein docking analyses indicate three possible modes of interaction with CLEC-2. All three modes result in a ligand-induced multimeric CLEC-2 signaling assembly on the surface of human platelets. These data contribute to our understanding of the rhodocytin-CLEC-2 interaction and its potential for inducing surface multimerization of CLEC-2. This study forms a basis for the rational investigation of ligand-induced CLEC-2 mediated platelet activation and aggregation in snake envenomation and vascular disease, and for the design of targeted therapies to block unwanted platelet aggregation.

Materials and Methods

Crystallization of rhodocytin and data collection

Rhodocytin was purified from the venom of *C. rhodostoma* as described previously (Eble et al. 2001) and concentrated to 9.5–15.5 mg/mL in 20 mM Tris pH 8.0, 150 mM NaCl. Crystallization screens were performed by vapor diffusion in nanoliter-scale sitting-drops using standard crystallization screening kits as implemented in the Oxford Protein Production Facility (Walter et al. 2005). Rhodocytin crystals selected for diffraction studies grew in 2 M ammonium sulfate, 5% 2-propanol. Crystals were frozen to 100K in a nitrogen cryostream using perfluoropolyether oil as a cryoprotectant. X-ray diffraction data to 2.4 Å resolution were collected from a single crystal mounted at the European Synchrotron Radiation Facility, Grenoble, France. The data collection strategy was implemented using the DNA system as part of the SPINE (structural proteomics in Europe) development of an automated structure-determination pipeline (Beteva et al. 2006). Two hundred sixty-three images were collected with an exposure time of 16.2 sec for each 0.4° oscillation. The data were autoindexed, integrated, and scaled using HKL2000 (Otwinowski and Minor 1997).

Rhodocytin structure determination

The structure of rhodocytin was solved using the molecular-replacement pipeline, BALBES (Long et al. 2008). The search models used were the C-type lectin-like molecules Factor X-binding protein (1IOD), Factor IX-binding protein (1J34), flavocetin-A (1C3A), and convulxin (1UMR). Subsequent manual rebuilding and refinement cycles used Coot and Refmac5 (Murshudov et al. 1997; Emsley and Cowtan 2004). Translation/libration/screw refinement parameters were included in the final stages of refinement (Winn et al. 2001). Residues in the structure are numbered according to their position relative to the amino termini of the α- and β-chains of the full-length protein as determined by N-terminal sequencing and verified by mass spectroscopy (Wang et al. 2001; Watson et al. 2007). The atomic coordinates and structure factors have been deposited with the Protein Data Bank (PDB entry 2VRP).

Computational dynamic analyses and docking studies

The Dynamite package was used to infer, analyze, and graphically represent the likely modes of motion of the α- and β-chains of rhodocytin (Barrett et al. 2004). Graphical representations of these dynamic analyses were generated with VMD (Humphrey et al. 1996). A model of the three-dimensional structure of a dimer of human CLEC-2 was manually assembled using Coot by superimposing two copies of the monomeric CLEC-2 structure (2C6U) onto the dimeric structure of the oxidized low density lipoprotein receptor LOX-1 (1YPQ), the most closely related dimeric C-type lectin-like structure. This dimeric CLEC-2 model was regularized and prepared for docking using energy minimization algorithms implemented by the Whatif server (Vriend 1990). Models of the rhodocytin crystal structure in complex with either monomeric or dimeric CLEC-2 were generated, filtered, and ranked using the Fourier transform correlation approach docking program Cluspro (Comeau et al. 2004). The most biologically plausible of these model complexes were selected on the basis of surface hydrophobicity, electrostatic compatibility, and the location of the CLEC-2 membrane insertion point. Electrostatic surface potentials were calculated using APBS, and images created using VMD, and PyMOL (DeLano Scientific) and rendered with Raster3D (Merritt and Murphy 1994; Baker et al. 2001). Surface areas were calculated with GetArea (Fraczkiewicz and Braun 1998).

Acknowledgments

This work was funded by the Medical Research Council and British Heart Foundation and is supported by the European Commission, LSHG-CT-2006-031220, SPINE2-COMPLEXES. J.A.E. is funded by the German Research Council (DFG grant: EB 177/5-1). We are grateful to Ben Hall, James Brown, and Steve Watson for useful discussions.

References

Baker, N.A., Sept, D., Joseph, S., Holst, M.J., and McCammon, J.A. 2001. Electrostatics of nanosystems: Application to microtubules and the ribosome. *Proc. Natl. Acad. Sci.* **98:** 10037–10041.

Barrett, C.P., Hall, B.A., and Noble, M.E. 2004. Dynamite: A simple way to gain insight into protein motions. *Acta Crystallogr. D Biol. Crystallogr.* **60:** 2280–2287.

Batuwangala, T., Leduc, M., Gibbins, J.M., Bon, C., and Jones, E.Y. 2004. Structure of the snake-venom toxin convulxin. *Acta Crystallogr. D Biol. Crystallogr.* **60:** 46–53.

Beteva, A., Cipriani, F., Cusack, S., Delageniere, S., Gabadinho, J., Gordon, E.J., Guijarro, M., Hall, D.R., Larsen, S., Launer, L., et al. 2006. High-throughput sample handling and data collection at synchrotrons: Embedding the ESRF into the high-throughput gene-to-structure pipeline. *Acta Crystallogr. D Biol. Crystallogr.* **62:** 1162–1169.

Brown, J.H. 2006. Breaking symmetry in protein dimers: Designs and functions. *Protein Sci.* **15:** 1–13.

Chippaux, J.P. 1998. Snake-bites: Appraisal of the global situation. *Bull. World Health Organ.* **76:** 515–524.

Christou, C.M., Pearce, A.C., Watson, A.A., Mistry, A.R., Pollitt, A.Y., Fenton-May, A.E., Johnson, L.A., Jackson, D.G., Watson, S.P., and O'Callaghan, C.A. 2008. Renal cells activate the platelet receptor CLEC-2 through podoplanin. *Biochem. J.* **411:** 133–140.

Comeau, S.R., Gatchell, D.W., Vajda, S., and Camacho, C.J. 2004. ClusPro: A fully automated algorithm for protein–protein docking. *Nucleic Acids Res.* **32:** W96–W99. doi: 10.1093/nar/gkh354.

Eble, J.A., Beermann, B., Hinz, H.J., and Schmidt-Hederich, A. 2001. $\alpha 2\ \beta\ 1$ integrin is not recognized by rhodocytin but is the specific, high affinity target of rhodocetin, an RGD-independent disintegrin and potent inhibitor of cell adhesion to collagen. *J. Biol. Chem.* **276:** 12274–12284.

Emsley, P. and Cowtan, K. 2004. Coot: Model-building tools for molecular graphics. *Acta Crystallogr. D Biol. Crystallogr.* **60:** 2126–2132.

Fraczkiewicz, R. and Braun, W. 1998. Exact and efficient analytical calculation of the accessible surface areas and their gradients for macromolecules. *J. Comput. Chem.* **19:** 319–333.

Fukuda, K., Mizuno, H., Atoda, H., and Morita, T. 2000. Crystal structure of flavocetin-A, a platelet glycoprotein Ib-binding protein, reveals a novel cyclic tetramer of C-type lectin-like heterodimers. *Biochemistry* **39:** 1915–1923.

Fuller, G.L., Williams, J.A., Tomlinson, M.G., Eble, J.A., Hanna, S.L., Pohlmann, S., Suzuki-Inoue, K., Ozaki, Y., Watson, S.P., and Pearce, A.C. 2007. The C-type lectin receptors CLEC-2 and Dectin-1, but not DC-SIGN, signal via a novel YXXL-dependent signaling cascade. *J. Biol. Chem.* **282:** 12397–12409.

Hirotsu, S., Mizuno, H., Fukuda, K., Qi, M.C., Matsui, T., Hamako, J., Morita, T., and Titani, K. 2001. Crystal structure of bitiscetin, a von Willebrand factor-dependent platelet aggregation inducer. *Biochemistry* **40:** 13592–13597.

Ho, M., Warrell, D.A., Looareesuwan, S., Phillips, R.E., Chanthavanich, P., Karbwang, J., Supanaranond, W., Viravan, C., Hutton, R.A., and Vejcho, S. 1986. Clinical significance of venom antigen levels in patients envenomed by the Malayan pit viper (*Calloselasma rhodostoma*). *Am. J. Trop. Med. Hyg.* **35:** 579–587.

Humphrey, W., Dalke, A., and Schulten, K. 1996. VMD: Visual molecular dynamics. *J. Mol. Graph.* **14:** 33–38.

Ji, T.H., Grossmann, M., and Ji, I. 1998. G protein-coupled receptors. I. Diversity of receptor-ligand interactions. *J. Biol. Chem.* **273:** 17299–17302.

Kato, K., Furihata, K., Cheli, Y., Radis-Baptista, G., and Kunicki, T.J. 2006. Effect of multimer size and a natural dimorphism on the binding of convulxin to platelet glycoprotein (GP)VI. *J. Thromb. Haemost.* **4:** 1107–1113.

Long, F., Vagin, A.A., Young, P., and Murshudov, G.N. 2008. BALBES: A molecular-replacement pipeline. *Acta Crystallogr. D Biol. Crystallogr.* **64:** 125–132.

Merritt, E.A. and Murphy, M.E. 1994. Raster3D Version 2.0. A program for photorealistic molecular graphics. *Acta Crystallogr. D Biol. Crystallogr.* **50:** 869–873.

Mizuno, H., Fujimoto, Z., Atoda, H., and Morita, T. 2001. Crystal structure of an anticoagulant protein in complex with the Gla domain of factor X. *Proc. Natl. Acad. Sci.* **98:** 7230–7234.

Mizuno, H., Fujimoto, Z., Koizumi, M., Kano, H., Atoda, H., and Morita, T. 1997. Structure of coagulation factors IX/X-binding protein, a heterodimer of C-type lectin domains. *Nat. Struct. Biol.* **4:** 438–441.

Murshudov, G.N., Vagin, A.A., and Dodson, E.J. 1997. Refinement of macromolecular structures by the maximum-likelihood method. *Acta Crystallogr. D Biol. Crystallogr.* **53:** 240–255.

Otwinowski, Z. and Minor, W. 1997. Processing of X-ray diffraction data collected in oscillation mode. *Methods Enzymol.* **276:** 307–326.

Shin, Y. and Morita, T. 1998. Rhodocytin, a functional novel platelet agonist belonging to the heterodimeric C-type lectin family, induces platelet aggregation independently of glycoprotein Ib. *Biochem. Biophys. Res. Commun.* **245:** 741–745.

Suzuki-Inoue, K., Fuller, G.L., Garcia, A., Eble, J.A., Pohlmann, S., Inoue, O., Gartner, T.K., Hughan, S.C., Pearce, A.C., Laing, G.D., et al. 2006. A novel Syk-dependent mechanism of platelet activation by the C-type lectin receptor CLEC-2. *Blood* **107:** 542–549.

Suzuki-Inoue, K., Kato, Y., Inoue, O., Kaneko, M.K., Mishima, K., Yatomi, Y., Yamazaki, Y., Narimatsu, H., and Ozaki, Y. 2007. Involvement of the snake toxin receptor CLEC-2, in podoplanin-mediated platelet activation, by cancer cells. *J. Biol. Chem.* **282:** 25993–26001.

Vriend, G. 1990. WHAT IF: A molecular modeling and drug design program. *J. Mol. Graph.* **8:** 52–56.

Walter, T.S., Diprose, J.M., Mayo, C.J., Siebold, C., Pickford, M.G., Carter, L., Sutton, G.C., Berrow, N.S., Brown, J., Berry, I.M., et al. 2005. A procedure for setting up high-throughput nanolitre crystallization experiments. Crystallization workflow for initial screening, automated storage, imaging and optimization. *Acta Crystallogr. D Biol. Crystallogr.* **61:** 651–657.

Wang, R., Kong, C., Kolatkar, P., and Chung, M.C. 2001. A novel dimer of a C-type lectin-like heterodimer from the venom of *Calloselasma rhodostoma* (Malayan pit viper). *FEBS Lett.* **508:** 447–453.

Watson, A.A. and O'Callaghan, C.A. 2005. Crystallization and X-ray diffraction analysis of human CLEC-2. *Acta Crystallogr. Sect. F Struct. Biol. Cryst. Commun.* **61:** 1094–1096.

Watson, A.A., Brown, J., Harlos, K., Eble, J.A., Walter, T.S., and O'Callaghan, C.A. 2007. The crystal structure and mutational binding analysis of the extracellular domain of the platelet-activating receptor CLEC-2. *J. Biol. Chem.* **282:** 3165–3172.

Winn, M.D., Isupov, M.N., and Murshudov, G.N. 2001. Use of TLS parameters to model anisotropic displacements in macromolecular refinement. *Acta Crystallogr. D Biol. Crystallogr.* **57:** 122–133.

Xie, J., Wu, T., Guo, L., Ruan, Y., Zhou, L., Zhu, H., Yun, X., Hong, Y., Jiang, J., Wen, Y., et al. 2008. Molecular characterization of two novel isoforms and a soluble form of mouse CLEC-2. *Biochem. Biophys. Res. Commun.* **371:** 180–184.